DALTON
FULL PAPER

Synthesis and reactivities of Ir_2Ru heterobimetallic sulfido clusters derived from a hydrogensulfido-bridged diiridium complex

Takuya Kochi,[a] Yasuo Nomura,[a] Zhen Tang,[a] Youichi Ishii,[a] Yasushi Mizobe[b] and Masanobu Hidai*[a]

[a] *Department of Chemistry and Biotechnology, Graduate School of Engineering, The University of Tokyo, Hongo, Bunkyo-ku, Tokyo 113-8656, Japan*
[b] *Institute of Industrial Science, The University of Tokyo, Roppongi, Minato-ku, Tokyo 106-8558, Japan. E-mail: hidai@chembio.t.u-tokyo.ac.jp*

Received 15th April 1999, Accepted 17th June 1999

The hydrogensulfido-bridged diiridium complex [ClCp*Ir(μ-SH)$_2$IrCp*Cl] reacted with [RuH$_2$(PPh$_3$)$_4$] to give a mixed-metal trinuclear cluster with an Ir$_2$Ru(μ$_3$-S)$_2$ core [(Cp*Ir)$_2$(μ$_3$-S)$_2$RuCl$_2$(PPh$_3$)] **2**, which was further converted into the cationic diphosphine derivatives [(Cp*Ir)$_2$(μ$_3$-S)$_2$RuCl(L)]Cl (L = dppe = Ph$_2$PCH$_2$CH$_2$PPh$_2$ **3** or depe = Et$_2$PCH$_2$CH$_2$PEt$_2$ **4**). The reaction of cluster **3** with Me$_2$CuLi followed by anion metathesis with KPF$_6$ afforded the cationic methyl cluster [(Cp*Ir)$_2$(μ$_3$-S)$_2$RuMe(dppe)][PF$_6$] **5** in good yield, while treatment of **3** with CHCl$_2$Li led to selective formation of [(Cp*Ir){(η^4-C$_5$Me$_5$CHCl$_2$)Ir}(μ$_3$-S)$_2$RuCl(dppe)] **6**, in which one of the Cp* ligands was alkylated by CHCl$_2$Li to form an η^4-diene. Clusters **3** and **4** were also transformed into the dihydrido clusters [(Cp*Ir)$_2$(μ$_3$-S)$_2$(μ-H)$_2$Ru(L)] (L = dppe **7** or depe **8**) by the reaction with NaBH$_4$. On the other hand, cluster **2** was converted into the carbonyl cluster [(Cp*Ir)$_2$(μ$_3$-S)$_2$RuCl(CO)(PPh$_3$)]Cl **9**, the isocyanide clusters [(Cp*Ir)$_2$(μ$_3$-S)$_2$RuCl(CNXy)(PPh$_3$)]Cl **10** (Xy = 2,6-C$_6$H$_3$Me$_2$) and [(Cp*Ir)$_2$(μ$_3$-S)$_2$Ru(CNXy)$_2$(PPh$_3$)][BPh$_4$]$_2$ **11** and the co-ordinatively unsaturated thiolato clusters [(Cp*Ir)$_2$(μ$_3$-S)$_2$Ru(SAr)$_2$] (Ar = 2,4,6-C$_6$H$_2$Pr$^i_3$ **12** or Xy **13**) on treatment with CO, XyNC and LiSAr, respectively. The molecular structures of [(Cp*Ir)$_2$(μ$_3$-S)$_2$RuCl(depe)][BPh$_4$] **4′**, **5**·CH$_2$Cl$_2$, **6**, **7** and **12**·2C$_6$H$_6$ were established by X-ray diffraction studies.

Transition-metal complexes with sulfur-based ligands have been attracting increasing interest,[1] primarily because they serve as models for biological systems[2] and industrial metal sulfide catalysts.[3] Complexes of metals relevant to such systems, most typically those of iron and molybdenum, have been extensively investigated. In contrast, the chemistry of noble metal complexes with sulfur ligands still remains much less exploited. With the intention of developing complexes with robust and reactive multimetallic sites, we have synthesized several types of multinuclear Group 8–10 noble metal complexes with sulfido or thiolato ligands.[4] In fact, intriguing transformations of various substrate molecules have been achieved on the multimetallic centres of, for example, [Cp*RuCl(μ-SPr^i)$_2$Ru(OH$_2$)Cp*][O$_3$SCF$_3$] (Cp* = η^5-C$_5$Me$_5$)[5] and [PdMo$_3$(μ$_3$-S)$_4$(tacn)$_3$Cl][PF$_6$]$_3$ (tacn = 1,4,7-triazacyclononane).[6] Inspired by these results, we have embarked on establishing a general and rational route for the construction of noble metal sulfido clusters with designed structures. Recently, we have newly synthesized a series of hydrogensulfido complexes [ClCp*M(μ-SH)$_2$MCp*Cl] (M = Ru,[7] Rh[8] or Ir[8]) and [Cp$_2$Ti(μ-SH)$_2$RuCp*Cl] (Cp = η^5-C$_5$H$_5$),[4d] and found that they can be used as versatile precursors for the syntheses of homo- and hetero-metallic sulfido clusters.[4c–e,7,8] In particular, the hydrogensulfido complex of iridium [ClCp*Ir(μ-SH)$_2$IrCp*Cl] **1** is transformed into various heterobimetallic clusters including trinuclear clusters with the triangular Ir$_2$M(μ$_3$-S)$_2$ core (M = Rh,[8a] Pd,[8a,c] Pt[8c] or Fe[4e]) and pentanuclear clusters with the bow-tie type Ir$_4$M(μ$_3$-S)$_4$ core (M = Fe, Co or Ni)[4e] by reaction with a second metal fragment. In addition, the trinuclear cluster [(Cp*Ir)$_2$(μ$_3$-S)$_2$PdCl$_2$] derived from **1** exhibits unique regioselectivity in the addition of alcohols to internal 1-aryl-1-alkynes.[8c] Now we have synthesized mixed-metal trinuclear clusters with an Ir$_2$Ru(μ$_3$-S)$_2$ core [(Cp*Ir)$_2$(μ$_3$-S)$_2$RuCl$_2$(PPh$_3$)] **2** and [(Cp*Ir)$_2$(μ$_3$-S)$_2$RuCl(L)]Cl (L = dppe = Ph$_2$PCH$_2$CH$_2$PPh$_2$ **3** or depe = Et$_2$PCH$_2$CH$_2$PEt$_2$ **4**) from complex **1**. Clusters **2**, **3** and **4** displayed interesting reactivities including regioselective alkylation of **3** either at the ruthenium centre or at the Cp* ligand.

Results and discussion

Preparation of the trinuclear cluster [(Cp*Ir)$_2$(μ$_3$-S)$_2$RuCl$_2$(PPh$_3$)] 2 and its diphosphine derivatives 3 and 4

Reaction of complex **1** with an almost equimolar amount of [RuH$_2$(PPh$_3$)$_4$] in thf smoothly took place at room temperature to give the mixed-metal trinuclear cluster **2** in good yield, eqn. (1). Evolution of H$_2$ gas (1.44 mol per **1**) during the reaction was confirmed by GLC analysis of the gaseous phase, suggesting that two molecules of H$_2$ were formed per one of cluster **2**. As a related reaction, we have recently reported that the diruthenium complex [ClCp*Ru(μ-SH)$_2$RuCp*Cl] reacts with [RuH$_2$(PPh$_3$)$_4$] to give a triruthenium cluster with a

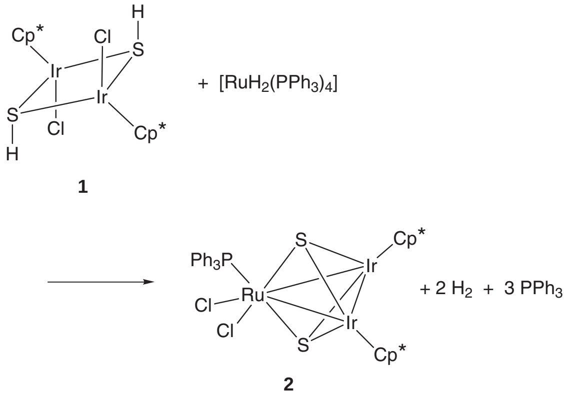

(1)

bridging hydrido ligand $[(Cp^*Ru)_2(\mu_3\text{-}S)_2(\mu\text{-}H)RuCl(PPh_3)_2]$.[4c] In the present reaction, however, cluster **2** was essentially the sole product detected by the ^1H NMR analysis of the crude reaction mixture, and formation of hydrido clusters was not observed. Cluster **2** could also be prepared from **1** and $[RuCl_2(PPh_3)_3]$, but the reaction was sluggish (23% conversion after 2 d at room temperature).

Cluster **2** was characterized by its ^1H and $^{31}P\text{-}\{^1H\}$ NMR spectra as well as the crystallographic study of its depe derivative described below. At room temperature, the ^1H NMR spectrum exhibited one Cp* singlet (δ 1.95) and aromatic signals due to the PPh_3 ligand with the intensity ratio of 2 : 1, while the $^{31}P\text{-}\{^1H\}$ NMR signal appeared as a broad singlet at δ 82.9. On lowering the temperature to −60 °C the Cp* signal in the ^1H NMR split into two singlets at δ 1.64 and 2.19 with the same intensities. This NMR behavior indicates that the favored conformer of the cluster at low temperatures has an unsymmetric structure where the PPh_3 ligand is located out of the RuS_2 plane, but the co-ordination around the ruthenium atom is fluxional at room temperature to make the two Cp* ligands apparently equivalent.

The Ir_2RuS_2 cluster core was further characterized as diphosphine derivatives. Thus, on treatment with dppe or depe, cluster **2** was converted into the cationic cluster **3** or **4**, respectively (Scheme 1), and the molecular structure of $[(Cp^*Ir)_2(\mu_3\text{-}S)_2RuCl(depe)][BPh_4]$ **4′**, the $[BPh_4]^-$ analogue of **4**, was unequivocally established by X-ray analysis. An ORTEP[9] drawing of the cation in **4′** is illustrated in Fig. 1, and selected bond distances and angles are listed in Table 1. Cluster **4′** has a triangular Ir_2Ru core capped by two μ_3-sulfido ligands from both sides. The two Ir–Ru contacts at 2.8922(9) and 2.8437(9) Å and the Ir–Ir contact at 2.7848(6) Å are consistent with Ir–Ru[10] and Ir–Ir[4e,11] single bonds, respectively. The Ru(1) atom is further co-ordinated by a chelating depe molecule and a chloro ligand, and if the two Ir–Ru bonds are neglected the geometry around the ruthenium atom is distorted trigonal bipyramidal with the S(1) and P(2) atoms at the apical positions. This geometry makes the molecule unsymmetric as a whole. The Ru(1)–S(1) distance [2.332(3) Å] is appreciably longer than Ru(1)–S(2) [2.261(3) Å] probably due to the *trans* influence of the P(2) atom. Although several $Ir_3(\mu_3\text{-}S)_2$[11c,d] and $Ru_3(\mu_3\text{-}S)_2$[4c,12] clusters with related structures have been reported, the mixed-metal $Ir_2Ru(\mu_3\text{-}S)_2$ core is unprecedented.

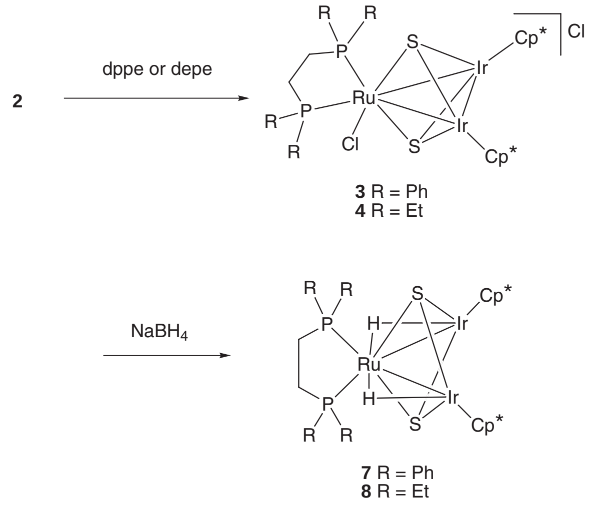

3 R = Ph
4 R = Et

7 R = Ph
8 R = Et

Scheme 1

At room temperature, each of complexes **3**, **4** and **4′** showed one Cp* signal (δ 1.88 for **3**; 2.11 for **4**; 1.99 for **4′**) in the ^1H NMR spectrum, although the cation in **4′** takes the unsymmetric solid state structure as described above. Their $^{31}P\text{-}\{^1H\}$ NMR spectra also displayed only one sharp singlet (δ 81.0 for **3**; 82.3 for **4** and **4′**). Furthermore, in contrast to cluster **2**, these cationic clusters exhibited no notable temperature dependence in the ^1H NMR spectra. Therefore, the cationic clusters **3** and **4** are considered to be much more fluxional than **2** with respect to the geometry around the ruthenium atom.

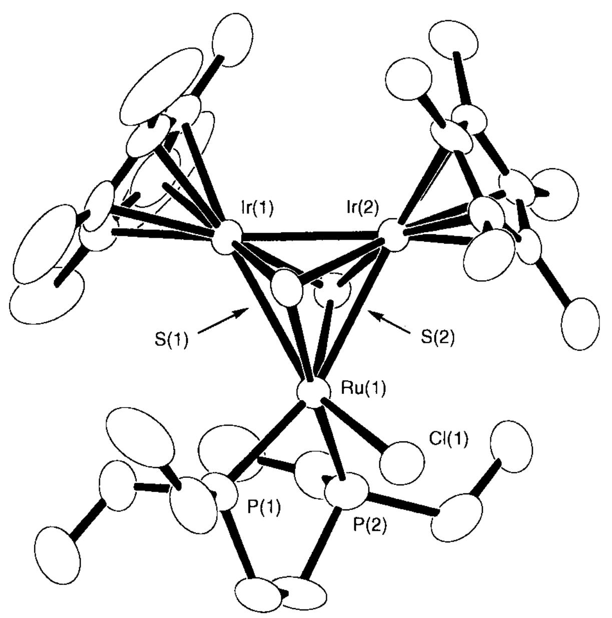

Fig. 1 Structure of the cationic part in complex **4′**. Hydrogen atoms are omitted for clarity. Thermal ellipsoids are shown at the 50% probability level.

Table 1 Selected interatomic distances (Å) and angles (°) in complex **4′**

Ir(1)–Ir(2)	2.7848(6)	Ir(1)–Ru(1)	2.8922(9)
Ir(2)–Ru(1)	2.8437(9)	Ir(1)–S(1)	2.285(3)
Ir(1)–S(2)	2.277(3)	Ir(2)–S(1)	2.291(3)
Ir(2)–S(2)	2.290(3)	Ru(1)–Cl(1)	2.392(3)
Ru(1)–S(1)	2.332(3)	Ru(1)–S(2)	2.261(3)
Ru(1)–P(1)	2.295(3)	Ru(1)–P(2)	2.313(3)
Ir(2)–Ir(1)–Ru(1)	60.08(2)	Ir(1)–Ir(2)–Ru(1)	61.83(2)
Ir(1)–Ru(1)–Ir(2)	58.08(2)	S(1)–Ir(1)–S(2)	88.90(9)
S(1)–Ir(2)–S(2)	88.41(9)	Cl(1)–Ru(1)–S(1)	91.80(10)
Cl(1)–Ru(1)–S(2)	134.8(1)	S(1)–Ru(1)–S(2)	88.11(9)
S(1)–Ru(1)–P(1)	101.5(1)	S(1)–Ru(1)–P(2)	176.9(1)
S(2)–Ru(1)–P(1)	139.4(1)	S(2)–Ru(1)–P(2)	89.7(1)

Regioselective alkylation reactions of cluster 3

Alkylation of cluster **3** was examined in detail. Although its reactions with MeLi, PhLi and MeMgBr ended in the formation of complex mixtures, selective methylation of the ruthenium centre was achieved by the reaction with Me_2CuLi at −20 °C. The ^1H NMR analysis of the crude product indicated the formation of a single cluster species, and the cationic methyl cluster $[(Cp^*Ir)_2(\mu_3\text{-}S)_2RuMe(dppe)][PF_6]\cdot CH_2Cl_2$ **5**·CH_2Cl_2 was isolated in 67% yield after anion metathesis with KPF_6 (Scheme 2). The ^1H NMR spectrum of cluster **5** exhibited one triplet at δ −1.14 [3 H, ^3J(PH) = 6.4 Hz] assignable to the RuMe protons and one singlet at δ 1.85 (30 H) due to the Cp* protons, both of which are consistent with the formulation. Attempted methylation of cluster **2** with Me_2CuLi did not give any isolable methyl clusters.

The molecular structure of complex **5**·CH_2Cl_2 was determined by X-ray analysis. An ORTEP drawing of the cation is given in Fig. 2, and important bond distances and angles are in Table 2. Cluster **5** has a triangular Ir_2Ru core capped by two μ_3-sulfido ligands, which is closely related to that of **4′**. The three metal–metal distances [Ir(1)–Ir(2), 2.7717(5); Ir(1)–Ru(1), 2.8695(8); Ir(2)–Ru(1), 2.978(1) Å] are diagnostic of metal–metal bonding interactions, where the elongation of the Ir(2)–Ru(1) bond is attributed to the steric congestion between the

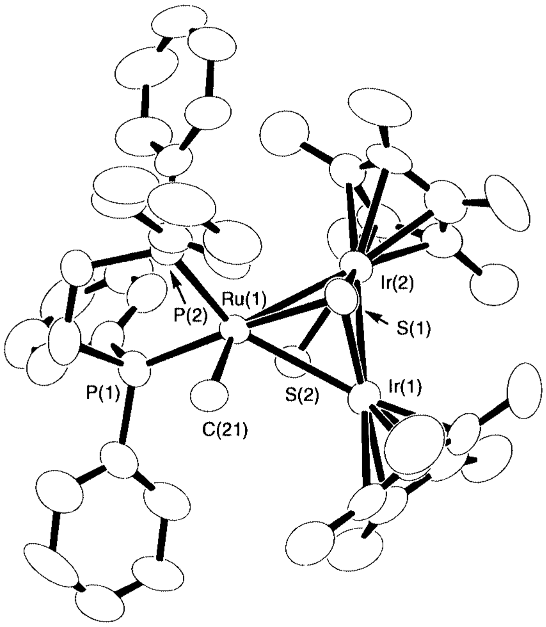

Fig. 2 Structure of the cationic part in complex **5**·CH_2Cl_2. Details as in Fig. 1.

Table 2 Selected interatomic distances (Å) and angles (°) in complex **5**·CH_2Cl_2

Ir(1)–Ir(2)	2.7717(5)	Ir(1)–Ru(1)	2.8695(8)
Ir(2)–Ru(1)	2.978(1)	Ir(1)–S(1)	2.284(3)
Ir(1)–S(2)	2.273(2)	Ir(2)–S(1)	2.288(2)
Ir(2)–S(2)	2.276(2)	Ru(1)–S(1)	2.328(2)
Ru(1)–S(2)	2.295(2)	Ru(1)–P(1)	2.266(3)
Ru(1)–P(2)	2.277(3)	Ru(1)–C(21)	2.147(9)
Ir(2)–Ir(1)–Ru(1)	63.71(2)	Ir(1)–Ir(2)–Ru(1)	59.74(2)
Ir(1)–Ru(1)–Ir(2)	56.55(2)	S(1)–Ir(1)–S(2)	87.70(9)
S(1)–Ir(2)–S(2)	87.52(8)	S(1)–Ru(1)–S(2)	86.10(9)
S(1)–Ru(1)–P(1)	176.05(10)	S(1)–Ru(1)–P(2)	100.24(9)
S(1)–Ru(1)–C(21)	95.4(3)	S(2)–Ru(1)–P(1)	91.75(9)
S(2)–Ru(1)–P(2)	146.86(9)	S(2)–Ru(1)–C(21)	125.9(3)

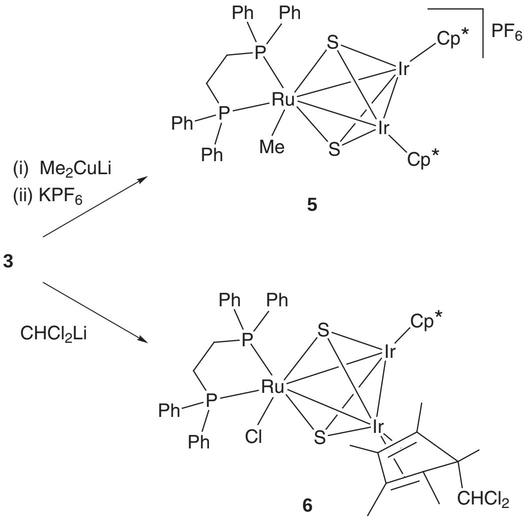

Scheme 2

phenyl groups on the P(2) atom and the Cp* ligand on the Ir(2) atom. It has unambiguously been confirmed that a methyl ligand [C(21)] is introduced onto the ruthenium centre. The geometry around the Ru(1) atom is distorted trigonal bipyramidal with the P(1) and S(1) atoms at the apical positions and the P(2), S(2) and C(21) atoms on the basal plane.

In contrast, treatment of cluster **3** with $CHCl_2Li$ led to formation of $[(Cp^*Ir)\{(\eta^4\text{-}C_5Me_5CHCl_2)Ir\}(\mu_3\text{-}S)_2RuCl(dppe)]$ **6**, which was isolated as dark brown crystals in 57% yield (Scheme 2). Formation of no other cluster species was observed by the ^1H NMR analysis of the crude reaction mixture, indicating that cluster **6** was produced quite selectively. The ^1H NMR spectrum of cluster **6** showed a set of singlets at δ 1.21 (3 H), 1.79 (6 H), 1.95 (6 H) and 5.23 (1 H) due to the η^4-$C_5Me_5CHCl_2$ ligand, which revealed that one of the Cp* ligands in **3** was alkylated by $CHCl_2Li$ to form the substituted η^4-cyclopentadiene ligand. This type of conversion of a Cp* ligand into a substituted η^4-cyclopentadiene ligand has been relatively rare.[13] Very recently, Tanaka *et al.*[13c] have reported that the trinuclear cluster $[(Cp^*Ir)_3(\mu_3\text{-}S)_2]$, which is generated by electrochemical reduction of $[(Cp^*Ir)_3(\mu_3\text{-}S)_2][BPh_4]_2$, reacts with MeCN under CO_2 to give a cationic cluster with a substituted η^4-cyclopentadiene ligand $[(Cp^*Ir)_2\{(\eta^4\text{-}C_5Me_5CH_2\text{-}CN)Ir\}(\mu_3\text{-}S)_2][BPh_4]$, although the reaction mechanism has not been clarified.

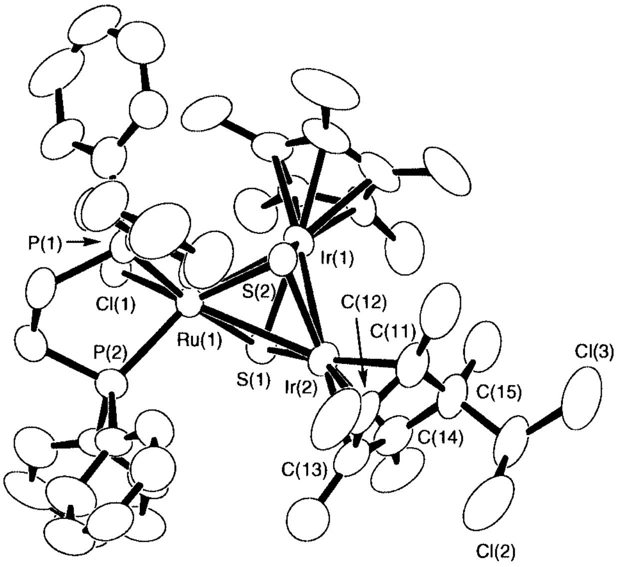

Fig. 3 Molecular structure of complex **6**. Details as in Fig. 1.

Table 3 Selected interatomic distances (Å) and angles (°) in complex **6**

Ir(1)–Ir(2)	2.8604(5)	Ir(1)–Ru(1)	2.8199(9)
Ir(2)–Ru(1)	2.9740(9)	Ir(1)–S(1)	2.294(2)
Ir(1)–S(2)	2.278(2)	Ir(2)–S(1)	2.285(2)
Ir(2)–S(2)	2.274(2)	Ir(2)–C(11)	2.159(10)
Ir(2)–C(12)	2.128(10)	Ir(2)–C(13)	2.13(1)
Ir(2)–C(14)	2.16(1)	Ru(1)–Cl(1)	2.428(2)
Ru(1)–S(1)	2.363(3)	Ru(1)–S(2)	2.296(2)
Ru(1)–P(1)	2.287(3)	Ru(1)–P(2)	2.274(3)
C(11)–C(12)	1.43(1)	C(11)–C(15)	1.52(1)
C(12)–C(13)	1.46(1)	C(13)–C(14)	1.41(1)
C(14)–C(15)	1.55(1)		
Ir(2)–Ir(1)–Ru(1)	63.14(2)	Ir(1)–Ir(2)–Ru(1)	57.77(2)
Ir(1)–Ru(1)–Ir(2)	59.10(2)	S(1)–Ir(1)–S(2)	87.61(8)
S(1)–Ir(2)–S(2)	87.92(9)	Cl(1)–Ru(1)–S(1)	89.33(8)
Cl(1)–Ru(1)–S(2)	136.12(9)	S(1)–Ru(1)–S(2)	85.55(8)
S(1)–Ru(1)–P(1)	173.32(9)	S(1)–Ru(1)–P(2)	103.44(9)
S(2)–Ru(1)–P(1)	90.71(9)	S(2)–Ru(1)–P(2)	141.38(10)
C(12)–C(11)–C(15)	108(1)	C(11)–C(12)–C(13)	106.0(10)
C(12)–C(13)–C(14)	107(1)	C(13)–C(14)–C(15)	108.0(9)
C(11)–C(15)–C(14)	95.5(8)		

The molecular structure of cluster **6** was further confirmed by X-ray diffraction study. An ORTEP drawing is illustrated in Fig. 3, and selected bond distances and angles are contained in Table 3. The metric features of the $Ir_2Ru(\mu_3\text{-}S)_2$ core in **6** are similar to those found in **5**·CH_2Cl_2 except that the Ir(1)–Ir(2) bond in **6** [2.8604(5) Å] is elongated. The η^4 co-ordination of the newly formed $C_5Me_5CHCl_2$ ligand with the Ir(2)–C bond distances at 2.128(10)–2.16(1) Å has been confirmed. The Ir(2) atom is now co-ordinated by the two sulfur atoms and the diene ligand with a square planar geometry. This structure suggests that the Ir(2) atom is reduced to the formal oxidation state of Ir^I on reaction with $CHCl_2Li$. On the other hand, the structure around the ruthenium atom is trigonal bipyramidal and closely related to that of cluster **4′**.

The diffraction study of complex **6** has also revealed that the $CHCl_2$ group in the η^4-$C_5Me_5CHCl_2$ ligand is located at the *exo* position. A mechanism consistent with the structure would involve direct nucleophilic attack of $CHCl_2Li$ at the Cp* ligand in the cationic cluster **3** from the outer co-ordination sphere,[13a,b] since indirect attack of a $CHCl_2$ group *via* the iridium centre to the Cp* ring is expected to lead to the *endo* η^4-$C_5Me_5CHCl_2$ isomer.[14] Alternatively, a mechanism involving the coupling of a $CHCl_2$ radical and the neutral cluster $[(Cp^*Ir)_2(\mu_3\text{-}S)_2\text{-}RuCl(dppe)]$ formed by one electron transfer between $CHCl_2Li$ and **3** may be operative.[15] It should be pointed out that the reaction site of **3** attacked by an alkylmetal reagent is highly dependent upon the nature of the reagent. We consider that soft and sterically small alkylmetals are driven to attack the ruthenium centre, while sterically demanding alkylmetals tend to attack the Cp* ligand.

Preparation of dihydrido clusters from 3 and 4

The regioselective alkylation reactions observed with cluster **3** led us to investigate the reactions of **2**, **3** and **4** with a hydride reagent for comparison. When cluster **3** was allowed to react with an excess amount of $NaBH_4$ in CH_2Cl_2–ethanol at room temperature the dihydrido cluster $[(Cp^*Ir)_2(\mu_3\text{-}S)_2(\mu\text{-}H)_2Ru\text{-}(dppe)]$ **7** was obtained in moderate yield (Scheme 1). Cluster **4** was analogously converted into the corresponding dihydrido cluster $[(Cp^*Ir)_2(\mu_3\text{-}S)_2(\mu\text{-}H)_2Ru(depe)]$ **8**. However, no characterizable hydrido cluster was obtained from **2**.

In the ^1H NMR spectrum cluster **7** exhibited a high-field hydrido resonance at δ −14.73 with the intensity of 2 H as a triplet by coupling with two equivalent phosphorus nuclei $[^2J(PH) = 13.4$ Hz$]$ as well as one Cp* signal at δ 1.97 (30 H). No temperature dependence was observed for these signals over the range 20 to −80 °C. The $^{31}P\text{-}\{^1H\}$ NMR spectrum also showed only one singlet, confirming the apparent equivalence of the phosphorus nuclei. The IR spectrum had no absorption in the range 1500–2200 cm^{-1} attributable to a terminal M–H stretching. Considering these spectral data, cluster **7** is deduced to have two hydrido ligands which bridge the two respective Ru–Ir edges. Cluster **8** showed a hydrido signal at δ −14.56 as a triplet $[^2J(PH) = 15.9$ Hz$]$ in the ^1H NMR spectrum but no IR absorption assignable to a terminal M–H stretching, revealing a structure similar to that of **7**.

The molecular structure of complex **7** was established by X-ray analysis. The unit cell contains two independent molecules, whose structures are essentially equivalent. An ORTEP drawing for one is depicted in Fig. 4, and important bond distances and angles are collected in Table 4. The Ir–Ru distances at an average of 2.803 Å are shorter than those found in clusters **4′**, **5**·CH_2Cl_2 and **6** and suggest that there exists substantial metal–metal bonding character between the ruthenium and iridium atoms. Although the positions of the hydrido ligands could not be determined crystallographically, each of these Ir–Ru edges is considered to be bridged by a hydrido ligand on the basis of the above mentioned spectroscopic data. The geometry around the ruthenium atom is viewed as distorted octahedral with the mutually *trans* μ-hydrido ligands, if the Ru–Ir interactions are neglected. On the other hand, the Ir–Ir separation in each independent cluster molecule [3.509(1), 3.568(2) Å] is much longer than those of **4′**, **5**·CH_2Cl_2 and **6** and is regarded to be non-bonding. The loss of the Ir–Ir bond makes the Ir–Ru–Ir bond angle [77.26(6), 79.31(6)°] significantly larger than the corresponding values found in **4′**, **5**·CH_2Cl_2 and **6** [56.55(2)–59.10(2)°]. The structure with the two metal–metal bonding contacts is in good agreement with the 50 valence electrons of **7**. As a related dihydrido cluster, we have recently synthesized $[(Cp^*Ru)_2(\mu_3\text{-}S)_2(\mu\text{-}H)RuH(PPh_3)_2]$ by treatment of $[(Cp^*Ru)_2(\mu_3\text{-}S)_2(\mu\text{-}H)RuCl(PPh_3)_2]$ with $NaBH_4$ and revealed its molecular structure with one terminal and one bridging hydrido ligand.[4c] In cluster **7** the large Ir–Ru–Ir angle probably enables both hydrido ligands to take bridging positions without deforming the H–Ru–H moiety from the ideal linear geometry.

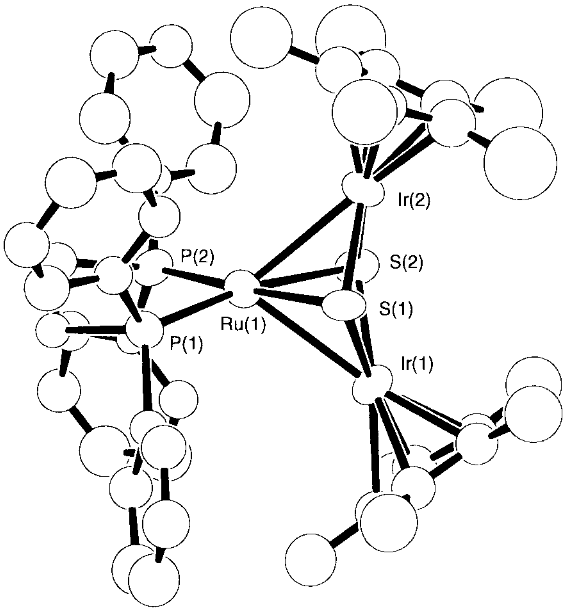

Fig. 4 Molecular structure of complex **7**. Details as in Fig. 1.

Table 4 Selected interatomic distances (Å) and angles (°) in complex **7**

Ir(1)···Ir(2)	3.509(1)	Ir(1)–Ru(1)	2.830(2)
Ir(2)–Ru(1)	2.790(2)	Ir(1)–S(1)	2.336(6)
Ir(1)–S(2)	2.336(7)	Ir(2)–S(1)	2.315(7)
Ir(2)–S(2)	2.288(6)	Ru(1)–S(1)	2.413(6)
Ru(1)–S(2)	2.393(6)	Ru(1)–P(1)	2.236(6)
Ru(1)–P(2)	2.242(6)		
Ir(3)···Ir(4)	3.568(2)	Ir(3)–Ru(2)	2.793(2)
Ir(4)–Ru(2)	2.798(2)	Ir(3)–S(3)	2.314(7)
Ir(3)–S(4)	2.307(6)	Ir(4)–S(3)	2.350(6)
Ir(4)–S(4)	2.352(6)	Ru(2)–S(3)	2.420(6)
Ru(2)–S(4)	2.397(6)	Ru(2)–P(3)	2.242(6)
Ru(2)–P(4)	2.230(6)		
Ir(1)–Ru(1)–Ir(2)	77.26(6)	S(1)–Ir(1)–S(2)	78.9(2)
S(1)–Ir(2)–S(2)	80.4(2)	S(1)–Ru(1)–S(2)	76.3(2)
S(1)–Ru(1)–P(1)	98.4(2)	S(1)–Ru(1)–P(2)	176.5(2)
S(2)–Ru(1)–P(1)	170.2(2)	S(2)–Ru(1)–P(2)	101.1(2)
Ir(3)–Ru(2)–Ir(4)	79.31(6)	S(3)–Ir(3)–S(4)	79.6(2)
S(3)–Ir(4)–S(4)	77.9(2)	S(3)–Ru(2)–S(4)	75.8(2)
S(3)–Ru(2)–P(3)	101.3(2)	S(3)–Ru(2)–P(4)	172.7(2)
S(4)–Ru(2)–P(3)	173.4(2)	S(4)–Ru(2)–P(4)	98.4(2)

Ligand substitution reactions of cluster 2

In addition to the reactions with diphosphine ligands, cluster **2** underwent several ligand substitution reactions. Treatment with CO (1 atm) at room temperature gave the cationic carbonyl cluster $[(Cp^*Ir)_2(\mu_3\text{-}S)_2RuCl(CO)(PPh_3)]Cl\cdot0.5CH_2Cl_2$ **9**·$0.5CH_2Cl_2$ (Scheme 3). The ^1H NMR spectrum showed a broad singlet due to the Cp* ligands at δ 2.14, and the IR spectrum one strong absorption assigned to the $\nu(CO)$ at 1929 cm^{-1}. No further reaction with CO took place even after a long time. In contrast, when **2** was allowed to react with XyNC (Xy = 2,6-$C_6H_3Me_2$), stepwise ligand substitution was observed. Thus, treatment of **2** with 1 equivalent of XyNC afforded the monocationic cluster $[(Cp^*Ir)_2(\mu_3\text{-}S)_2RuCl(CNXy)(PPh_3)]Cl$ **10**, whereas the ^1H NMR analysis of the reaction mixture obtained

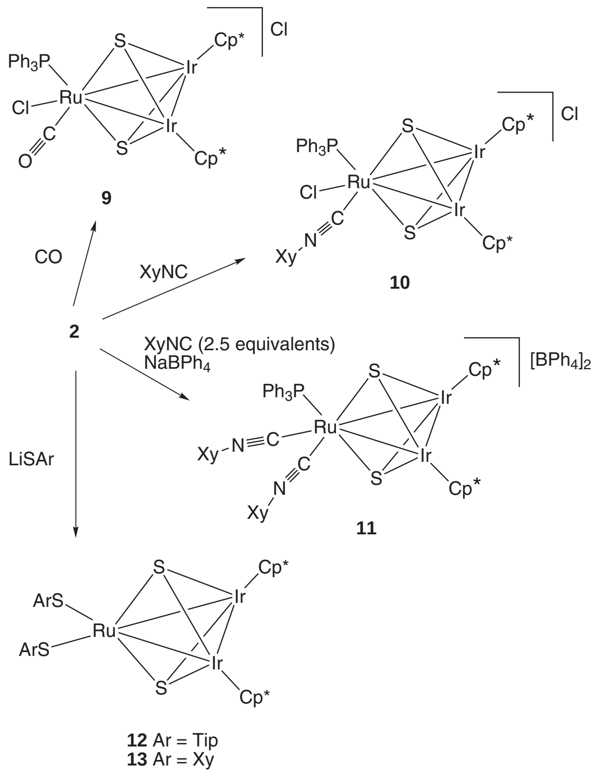

Scheme 3

by treatment of **2** with 2.5 equivalents of XyNC suggested that both of the chloro ligands in **2** were substituted by the XyNC ligands. Anion metathesis of the latter product with $NaBPh_4$ led to isolation of the dicationic cluster $[(Cp^*Ir)_2(\mu_3\text{-}S)_2Ru(CNXy)_2(PPh_3)][BPh_4]_2\cdot CH_2Cl_2$ **11**$\cdot CH_2Cl_2$. Cluster **10** exhibited one IR band attributable to the ν(CN) at 2054 cm^{-1}. On the other hand, two ν(CN) bands were observed with cluster **11** at higher wavenumbers (2106 and 2135 cm^{-1}), reflecting its dicationic nature.

During the above reactions with CO and XyNC the PPh_3 ligand on the ruthenium atom in complex **2** remains intact. However, substitution of the two chloro ligands on the ruthenium centre by more bulky anionic ligands is expected to give co-ordinatively unsaturated clusters by sterically induced dissociation of the PPh_3 ligand. Actually, reactions of cluster **2** with lithium salts of sterically demanding 2,6-substituted arenethiolate anions such as $TipS^-$ (Tip = 2,4,6-$C_6H_2Pr^i_3$) and XyS^- yielded $[(Cp^*Ir)_2(\mu_3\text{-}S)_2Ru(SAr)_2]$ (Ar = Tip **12** or Xy **13**) (Scheme 3).

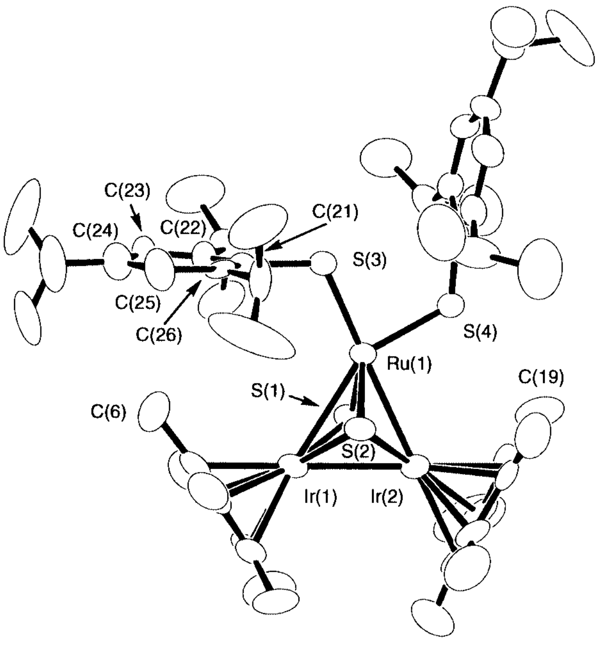

Fig. 5 Molecular structure of complex **12**$\cdot 2C_6H_6$. Solvating benzene molecules and hydrogen atoms are omitted for clarity. Thermal ellipsoids are shown at the 50% probability level.

Table 5 Selected interatomic distances (Å) and angles (°) in complex **12**$\cdot 2C_6H_6$

Ir(1)–Ir(2)	2.7518(8)	Ir(1)–Ru(1)	2.976(1)
Ir(2)–Ru(1)	2.833(1)	Ir(1)–S(1)	2.283(4)
Ir(1)–S(2)	2.285(4)	Ir(2)–S(1)	2.275(5)
Ir(2)–S(2)	2.279(5)	Ru(1)–S(1)	2.223(4)
Ru(1)–S(2)	2.202(4)	Ru(1)–S(3)	2.276(3)
Ru(1)–S(4)	2.271(4)		
Ir(2)–Ir(1)–Ru(1)	59.14(3)	Ir(1)–Ir(2)–Ru(1)	64.38(3)
Ir(1)–Ru(1)–Ir(2)	56.48(3)	Ir(1)–Ru(1)–S(3)	123.69(10)
Ir(2)–Ru(1)–S(4)	92.7(1)	S(1)–Ir(1)–S(2)	84.7(1)
S(1)–Ir(2)–S(2)	85.0(1)	S(1)–Ru(1)–S(2)	88.1(1)
S(1)–Ru(1)–S(3)	134.5(2)	S(1)–Ru(1)–S(4)	107.9(2)
S(2)–Ru(1)–S(3)	122.0(2)	S(2)–Ru(1)–S(4)	118.9(2)
S(3)–Ru(1)–S(4)	87.8(1)		

The molecular structure of complex **12**$\cdot 2C_6H_6$ disclosed by X-ray diffraction study is illustrated in Fig. 5, and selected bond distances and angles are collected in Table 5. The trinuclear core with three metal–metal bonds and two μ_3-S ligands is retained. Although this cluster has 46 valence electrons and can be regarded as co-ordinatively unsaturated, the structure of the $Ir_2Ru(\mu_3\text{-}S)_2$ core is very close to that of the $48e^-$ cluster **5** except that the Ru–(μ_3-S) bond distances in **12**$\cdot 2C_6H_6$ [2.202(4), 2.223(4) Å] are shorter by 0.09–0.10 Å. The ruthenium atom is tetrahedrally co-ordinated by the four sulfur atoms, and the three metal atoms and the two sulfur atoms of the STip ligands are nearly coplanar. The two aromatic rings of the Tip groups are oriented almost perpendicular to this Ir_2RuS_2 plane (dihedral angles, 88.4 and 80.3°). Interestingly, the STip ligands are arranged in a highly unsymmetric conformation. Thus, the Tip group attached to the S(4) atom is directed away from the $(Cp^*Ir)_2(\mu_3\text{-}S)_2$ moiety, while that connected to the S(3) atom is located close to the Cp* ligand on the Ir(1) atom. At the same time, the Ir(1)–Ru(1)–S(3) angle [123.69(10)°] is significantly larger than the Ir(2)–Ru(1)–S(4) angle [92.7(1)°]. This characteristic conformation minimizes the steric congestion between the STip ligands and the Cp* ligands. In fact, unusually short non-bonding contacts are observed between the S(4) and C(19) (Cp* methyl) atoms (3.48 Å) and between the C(6) (Cp* methyl) atom and the C(21)–C(26) aromatic ring (3.43 Å), both of which are shorter than the sums of the van der Waals radii of a methyl group (2.0 Å) and a sulfur (1.85 Å) or aromatic carbon atom (1.7 Å).[16] In particular, the latter distance suggests the presence of an attractive interaction between the methyl group and the aromatic ring, *i.e.*, CH · · · π interaction.[17]

The ^1H NMR spectrum of complex **12** showed notable temperature dependence. At room temperature one broad signal at δ 1.99 attributable to Cp* ligands was observed, which split into two broad signals at δ 1.63 and 2.27 on cooling at −40 °C. This behavior can be accounted for by considering the conformational interchange of the STip ligands which are arranged in an unsymmetric structure as disclosed by the crystallographic study, eqn. (2).

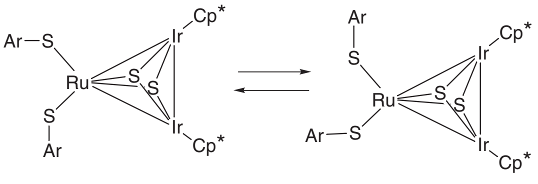

(2)

Conclusion

We have synthesized novel mixed-metal sulfido clusters **2**, **3** and **4** with the $Ir_2Ru(\mu_3\text{-}S)_2$ core by using the dinuclear hydrogensulfido complex **1** as the synthetic precursor. These clusters exhibited various reactivities including the regioselective alkylation of cluster **3** at either the ruthenium centre or the Cp* ligand. Clusters **5**, **6**, **7** and **8** have relatively labile or reactive ligands such as methyl, diene and hydrido ligands, and further reactions of these clusters as well as of the unsaturated clusters **12** and **13** are now under investigation.

Experimental

All manipulations were carried out under an atmosphere of nitrogen by the use of standard Schlenk tube techniques. Solvents were dried by common procedures and distilled before use. Complex **1**,[8a,b] $[RuH_2(PPh_3)_4]$,[18] $[RuCl_2(PPh_3)_3]$[19] and TipSH[20] were prepared according to literature methods. Lithium thiolates were prepared by reactions of Bu^{n}Li with the corresponding thiols. Other reagents were commercially obtained and used as received. The IR spectra were recorded on a Shimadzu 8100M spectrometer, ^{1}H (270 MHz) and ^{31}P-{^{1}H} NMR (109 MHz) spectra on a JEOL EX-270 spectrometer. Hydrogen gas evolution was determined by GLC analysis using a Shimadzu GC-8A gas chromatograph equipped with a molecular sieve 13X column. Elemental analyses were performed on a Perkin-Elmer 2400II CHN analyser. Amounts of the solvent molecules in the crystals were determined not only by elemental analyses but also by ^{1}H NMR spectroscopy.

Preparations

$[(Cp^*Ir)_2(\mu_3\text{-}S)_2RuCl_2(PPh_3)]\cdot 0.25thf$ 2·0.25thf. To a suspension of complex **1** (1.01 g, 1.28 mmol) in thf (30 cm^3) was added $[RuH_2(PPh_3)_4]$ (1.75 g, 1.52 mmol), and the mixture stirred at room temperature for 20 h. The resulting dark brown solution was concentrated to 2 cm^3, and the dark brown microcrystals deposited were collected by filtration and washed with hexane to give the trinuclear cluster **2**·0.25thf (1.36 g, 1.16 mmol, 91% yield) (Found: C, 40.09; H, 4.05. $C_{39}H_{47}Cl_2Ir_2O_{0.25}PRuS_2$ requires C, 39.99; H, 4.04%). $\delta_H(CDCl_3)$ 1.95 (30 H, s, Cp*), 7.28 (9 H, br, Ph) and 7.70 (6 H, br, Ph). $\delta_P(CDCl_3)$ 82.9 (br s). In a separate run the GLC analysis of the gaseous phase indicated that H_2 gas (1.44 mol per complex **1**) was evolved during the reaction.

$[(Cp^*Ir)_2(\mu_3\text{-}S)_2RuCl(dppe)]Cl$ 3. To a suspension of complex **2**·0.25thf (2.00 g, 1.71 mmol) in thf (200 cm^3) was added dppe (1.05 g, 2.64 mmol), and the mixture stirred at room temperature for 18 h. The resulting solution was concentrated to 10 cm^3, and a dark brown powder deposited was collected by filtration and washed with diethyl ether to give **3** (1.96 g, 1.52 mmol, 89% yield) (Found: C, 42.64; H, 4.30. $C_{46}H_{54}Cl_2Ir_2P_2RuS_2$ requires C, 42.85; H, 4.22%). $\delta_H(CDCl_3)$ 1.88 (30 H, s, Cp*), 2.25–2.40, 3.03–3.14 (2 H each, m, CH_2) and 7.15–7.84 (20 H, m, Ph). $\delta_P(CDCl_3)$ 81.0 (s).

$[(Cp^*Ir)_2(\mu_3\text{-}S)_2RuCl(depe)]Cl$ 4. This complex was prepared from **2**·0.25thf and depe by a similar procedure to that described for **3** and isolated in 81% yield as a dark brown powder (Found: C, 32.78; H, 4.99. $C_{30}H_{54}Cl_2Ir_2P_2RuS_2$ requires C, 32.84; H, 4.96%). $\delta_H(CDCl_3)$ 1.06 [6 H, dt, ^3J(PH) 14.5, ^3J(HH) 7.6, CH_2*Me*], 1.27 [6 H, dt, ^3J(PH) 17.2, ^3J(HH) 7.6 Hz, CH_2*Me*], 1.43–1.54 (2 H, m, CH_2), 1.75–1.94 (6 H, m, CH_2), 1.98–2.16 (4 H, m, CH_2) and 2.11 (30 H, s, Cp*). $\delta_P(CDCl_3)$ 82.3 (s).

$[(Cp^*Ir)_2(\mu_3\text{-}S)_2RuCl(depe)][BPh_4]$ 4′. To a suspension of complex **4** (50 mg, 0.046 mmol) in thf (10 cm^3) was added $NaBPh_4$ (78 mg, 0.23 mmol), and the mixture stirred at room temperature for 24 h. The solvent was removed *in vacuo*, and the residual solid extracted with CH_2Cl_2. The CH_2Cl_2 solution was concentrated to 5 cm^3 and thf (0.3 cm^3) added. Slow diffusion of hexane (10 cm^3) into the solution afforded **4′** (6 mg, 0.004 mmol, 10% yield) as dark brown crystals (Found: C, 47.06; H, 5.53. $C_{54}H_{74}BClIr_2P_2RuS_2$ requires C, 46.96; H, 5.40%). $\delta_H(CDCl_3)$ 1.00 [6 H, dt, ^3J(PH) 14.5, ^3J(HH) 7.6, CH_2*Me*], 1.25 [6 H, dt, ^3J(PH) 17.2, ^3J(HH) 7.6, CH_2*Me*], 1.35–1.48 (2 H, m, CH_2), 1.66–1.90 (6 H, m, CH_2), 1.99 (30 H, s, Cp*), 2.05–2.12 (4 H, m, CH_2), 6.87 [4 H, t, ^3J(HH) 7.3, BPh_4], 7.03 [8 H, t, ^3J(HH) 7.4 Hz, BPh_4] and 7.38–7.44 (8 H, m, BPh_4). $\delta_P(CDCl_3)$ 82.3 (s).

$[(Cp^*Ir)_2(\mu_3\text{-}S)_2RuMe(dppe)][PF_6]\cdot CH_2Cl_2$ 5·CH$_2$Cl$_2$. To a thf (20 cm^3) solution of Me_2CuLi prepared from CuI (111 mg, 0.58 mmol) and MeLi (1.16 mmol, in ether) at −20 °C was added complex **3** (500 mg, 0.388 mmol) at this temperature, and the mixture kept at −20 °C for 1.5 h with stirring. Hexane (50 cm^3) was added dropwise to the resulting dark brown mixture, and the dark brown powder precipitated was collected by filtration, washed with hexane and dried *in vacuo*. This crude product was dissolved in thf (30 cm^3) and KPF_6 (714 mg, 3.88 mmol) added. The mixture was stirred at room temperature for 15 h and the solvent then removed *in vacuo*. The resulting dark brown solid was extracted with CH_2Cl_2. Addition of hexane to the concentrated CH_2Cl_2 solution afforded **5**·CH_2Cl_2 (383 mg, 0.262 mmol, 67% yield) as dark brown crystals (Found: C, 39.28; H, 3.99. $C_{48}H_{59}Cl_2F_6Ir_2P_3RuS_2$ requires C, 39.39; H, 4.06%). $\delta_H(CDCl_3)$ −1.14 [3 H, t, ^3J(PH) 6.4 Hz, RuMe], 1.85 (30 H, s, Cp*), 2.12–2.34 (2 H, m, CH_2), 2.72–2.90 (2 H, m, CH_2) and 7.15–7.82 (20 H, m, Ph). $\delta_P(CDCl_3)$ 83.2 (s).

$[(Cp^*Ir)\{(\eta^4\text{-}C_5Me_5CHCl_2)Ir\}(\mu_3\text{-}S)_2RuCl(dppe)]$ 6. To a thf (20 cm^3) solution of $CHCl_2Li$ prepared from CH_2Cl_2 (19 mg, 0.22 mmol) and Bu^{n}Li (0.22 mmol, in ether) at −78 °C was added complex **3** (100 mg, 0.078 mmol) at this temperature. The mixture was slowly warmed to room temperature with stirring. The solvent was evaporated to dryness, and the residual dark brown solid extracted with benzene. The benzene was removed *in vacuo*, and the residue dissolved in thf. Addition of hexane to the concentrated thf solution formed a small amount of dark brown crystals of **6** and a brown powder, the latter of which was filtered off. The brown filtrate was concentrated to give **6** (59 mg, 0.044 mmol, 57% yield) as dark brown microcrystals (Found: C, 42.59; H, 4.27. $C_{47}H_{55}Cl_3Ir_2P_2RuS_2$ requires C, 42.19; H, 4.14%). $\delta_H(C_6D_6)$ 1.21 (3 H, s, Me), 1.75 (15 H, s, Cp*), 1.79 (6 H, s, Me), 1.83–2.05 (2 H, m, CH_2), 1.95 (6 H, s, Me), 2.86–3.08 (2 H, m, CH_2), 5.23 (1 H, s, $CHCl_2$) and 7.00–8.21 (20 H, m, Ph). $\delta_P(C_6D_6)$ 81.0 (s).

$[(Cp^*Ir)_2(\mu_3\text{-}S)_2(\mu\text{-}H)_2Ru(dppe)]$ 7. To a solution of complex **3** (499 mg, 0.387 mmol) in CH_2Cl_2 (30 cm^3)–ethanol (70 cm^3) was added $NaBH_4$ (101 mg, 2.67 mmol) in small portions, and the mixture stirred at room temperature for 45 h. The resulting dark brown solution was evaporated to dryness, and the residue extracted with benzene. The benzene was removed *in vacuo* and the dark brown residue recrystallized from thf–hexane to give **7** (198 mg, 0.162 mmol, 42% yield) as a dark brown powder (Found: C, 45.52; H, 4.79. $C_{46}H_{56}Ir_2P_2RuS_2$ requires C, 45.27; H, 4.62%). $\delta_H(C_6D_6)$ −14.73 [2 H, t, ^2J(PH) 13.4, hydrido], 1.97 (30 H, s, Cp*), 2.78 [4 H, d, ^2J(PH) 17.8 Hz, CH_2] and 7.02–7.73 (20 H, m, Ph). $\delta_P(C_6D_6)$ 73.6 (s).

$[(Cp^*Ir)_2(\mu_3\text{-}S)_2(\mu\text{-}H)_2Ru(depe)]$ 8. To a solution of complex **4** (200 mg, 0.182 mmol) in CH_2Cl_2 (10 cm^3)–ethanol (5 cm^3) was added $NaBH_4$ (69 mg, 1.8 mmol) in small portions, and the mixture stirred at room temperature for 16 h. The resulting dark brown solution was evaporated to dryness and the residue extracted with hexane. Evaporation of the solvent to dryness gave essentially pure **8** (100 mg, 0.097 mmol, 53% yield) as a

Table 6 X-Ray crystallographic data for complexes **4′**, **5**·CH$_2$Cl$_2$, **6**, **7** and **12**·2C$_6$H$_6$

	4′	**5**·CH$_2$Cl$_2$	**6**	**7**	**12**·2C$_6$H$_6$
Formula	$C_{54}H_{74}BClIr_2P_2RuS_2$	$C_{48}H_{59}Cl_2F_6Ir_2P_3RuS_2$	$C_{47}H_{55}Cl_3Ir_2P_2RuS_2$	$C_{46}H_{56}Ir_2P_2RuS_2$	$C_{62}H_{88}Ir_2RuS_4$
M	1381.02	1463.44	1337.89	1220.53	1447.13
Crystal system	Monoclinic	Monoclinic	Monoclinic	Monoclinic	Monoclinic
Space group	$P2_1/a$	$P2_1/n$	$P2_1/c$	$P2_1$	$P2_1$
a/Å	17.451(3)	11.460(3)	12.287(2)	17.369(2)	12.081(2)
b/Å	17.774(4)	12.065(4)	15.247(2)	14.609(1)	16.767(3)
c/Å	17.776(3)	37.612(3)	25.921(2)	17.631(4)	15.752(2)
β/°	97.66(1)	94.31(2)	94.10(1)	90.26(1)	91.66(1)
U/Å^3	5464(1)	5185(2)	4843(1)	4473(1)	3189.4(8)
Z	4	4	4	4	2
μ(Mo-Kα)/cm^{-1}	53.63	57.52	61.54	64.80	45.73
Independent reflections	12549 (R_{int} = 0.046)	9033 (R_{int} = 0.043)	8528 (R_{int} = 0.029)	10679 (R_{int} = 0.043)	5825 (R_{int} = 0.025)
Final *R*, *R′* [$I > 3.0\sigma(I)$]	0.048, 0.032	0.041, 0.042	0.038, 0.025	0.057, 0.039	0.041, 0.027

dark brown powder (Found: C, 35.39; H, 5.47. $C_{30}H_{56}Ir_2P_2RuS_2$ requires C, 35.04; H, 5.49%). δ_H(C$_6$D$_6$) −14.56 [2 H, t, ^2J(PH) 15.9, hydrido], 1.10 [12 H, dt, ^3J(PH) 14.7, ^3J(HH) 7.6 Hz, CH$_2$*Me*], 1.59–1.80 (12 H, m, CH$_2$) and 2.07 (30 H, s, Cp*). δ_P(C$_6$D$_6$) 79.6 (s).

[(Cp*Ir)$_2$(μ_3-S)$_2$RuCl(CO)(PPh$_3$)]Cl·0.5CH$_2$Cl$_2$ 9·0.5CH$_2$Cl$_2$. A CH$_2$Cl$_2$ (5 cm^3) solution of complex **2**·0.25thf (49 mg, 0.042 mmol) was stirred under an atmosphere of CO at room temperature for 2 h. Then the solution was concentrated under reduced pressure, and hexane added to the resultant solution to give **9**·0.5CH$_2$Cl$_2$ (42 mg, 0.034 mmol, 82% yield) as dark red needles (Found: C, 38.50; H, 4.00. $C_{39.5}H_{46}Cl_3Ir_2OPRuS_2$ requires C, 38.77; H, 3.79%). δ_H(CDCl$_3$) 2.14 (30 H, s, Cp*) and 7.40–7.57 (15 H, m, Ph). δ_P(CDCl$_3$) 40.5 (s). $\tilde{\nu}_{max}$/cm^{-1} (CO) 1929 (KBr).

[(Cp*Ir)$_2$(μ_3-S)$_2$RuCl(CNXy)(PPh$_3$)]Cl 10. A mixture of complex **2**·0.25thf (93 mg, 0.079 mmol) and XyNC (11 mg, 0.083 mmol) in CH$_2$Cl$_2$ (5 cm^3) was stirred at room temperature for 20 h. The reaction mixture was filtered and concentrated under reduced pressure. Addition of hexane to the concentrated solution afforded **10** (82 mg, 0.064 mmol, 80% yield) as a dark brown solid (Found: C, 43.58; H, 4.24; N, 0.84. $C_{47}H_{54}Cl_2Ir_2NPRuS_2$ requires C, 43.95; H, 4.24; N, 1.09%). δ_H(CDCl$_3$) 2.05 (6 H, s, *o*-Me), 2.11 (30 H, s, Cp*), 7.00 (3 H, br, Ar) and 7.34–7.53 (15 H, m, PPh$_3$). δ_P(CDCl$_3$) 43.0 (s). $\tilde{\nu}_{max}$/cm^{-1} (CN) 2054 (KBr).

[(Cp*Ir)$_2$(μ_3-S)$_2$Ru(CNXy)$_2$(PPh$_3$)][BPh$_4$]$_2$·CH$_2$Cl$_2$ 11·CH$_2$Cl$_2$. A mixture of complex **2**·0.25thf (100 mg, 0.085 mmol), XyNC (28 mg, 0.21 mmol) and NaBPh$_4$ (292 mg, 0.853 mmol) in CH$_2$Cl$_2$ (5 cm^3) was stirred at room temperature for 15 h. The reaction mixture was filtered and concentrated, and addition of ether afforded **11**·CH$_2$Cl$_2$ (111 mg, 0.054 mmol, 63% yield) as a reddish brown powder (Found: C, 61.03; H, 5.10; N, 1.57. $C_{105}H_{105}B_2Cl_2Ir_2N_2PRuS_2$ requires C, 60.98; H, 5.12; N, 1.35%). δ_H(CD$_2$Cl$_2$) 1.91 (30 H, s, Cp*), 2.04 (12 H, s, *o*-Me) and 6.80–7.51 (61 H, m, Ar). δ_P(CD$_2$Cl$_2$) 45.0 (s). $\tilde{\nu}_{max}$/cm^{-1} (CN) 2106 and 2135 (KBr).

[(Cp*Ir)$_2$(μ_3-S)$_2$Ru(STip)$_2$] 12. A mixture of complex **2**·0.25thf (102 mg, 0.087 mmol) and LiSTip (83 mg, 0.34 mmol) in thf (8 cm^3) was stirred at room temperature for 15 h. Then the solvent was evaporated to dryness, and the residue extracted with benzene. Addition of MeOH to the concentrated benzene solution afforded crystals of **12**·2C$_6$H$_6$ which were used for crystallographic study. The crystals gave off benzene on drying under vacuum to give **12** (78 mg, 0.060 mmol, yield 69%) as a dark brown solid (Found: C, 46.43; H, 6.01. $C_{50}H_{76}Ir_2RuS_4$ requires C, 46.52; H, 5.93%). δ_H(CDCl$_3$) 1.13 [24 H, d, ^3J(HH) 6.9, *o*-CH*Me*$_2$], 1.19 [12 H, d, ^3J(HH) 6.9, *p*-CH*Me*$_2$], 1.99 (30 H, br s, Cp*), 2.71 [2 H, sep, ^3J(HH) 6.9, *p*-C*H*Me$_2$], 3.85 [4 H, sep, ^3J(HH) 6.9 Hz, *o*-C*H*Me$_2$] and 6.75 (4 H, s, Ar).

[(Cp*Ir)$_2$(μ_3-S)$_2$Ru(SXy)$_2$] 13. A mixture of complex **2**·0.25thf (104 mg, 0.089 mmol) and LiSXy (56 mg, 0.39 mmol) in thf (8 cm^3) was stirred at room temperature for 15 h. The solvent was evaporated to dryness and the residue extracted with thf. Addition of hexane to the concentrated thf solution afforded **13** (10 mg, 0.009 mmol, 10% yield) as dark brown plates (Found: C, 39.86; H, 4.61. $C_{36}H_{48}Ir_2RuS_4$ requires C, 39.50; H, 4.42%). δ_H(CDCl$_3$) 1.97 (30 H, br s, Cp*), 2.17 (12 H, br, *o*-Me) and 6.90 (6 H, br, Ar).

Crystallography

Crystallographic data for complexes **4′**, **5**·CH$_2$Cl$_2$, **6**, **7** and **12**·2C$_6$H$_6$ are summarized in Table 6. Diffraction data were collected on a Rigaku AFC7R four-circle automated diffractometer at 294 K with graphite-monochromatized Mo-Kα radiation (λ = 0.71069 Å) using the ω–2θ scan technique for **4′**, **7** and **12**·2C$_6$H$_6$ and the ω scan technique for **5**·CH$_2$Cl$_2$ and **6**.

The structure solution and refinements were carried out by using the TEXSAN crystallographic software package.[21] The positions of the non-hydrogen atoms were determined by Patterson methods (DIRDIF PATTY[22]) and subsequent Fourier syntheses. All non-hydrogen atoms were refined by full-matrix least-squares techniques (based on *F*) with anisotropic thermal parameters except for the carbon atoms of the CH$_2$Cl$_2$ molecule in **5**·CH$_2$Cl$_2$, cluster **7** and the C$_6$H$_6$ molecules in **12**·2C$_6$H$_6$. The carbon atoms of **7** were refined with isotropic parameters, while fixed parameters were used for the carbon atoms of the solvent molecules in **5**·CH$_2$Cl$_2$ and **12**·2C$_6$H$_6$. Hydrogen atoms except for those of the CH$_2$Cl$_2$ molecule in **5**·CH$_2$Cl$_2$ and the hydrido ligands in **7** were placed at calculated positions (d_{C-H} = 0.95 Å) and included with fixed isotropic parameters. For **7** and **12**·2C$_6$H$_6$, the Flack absolute structure parameters[23] were close to zero [−0.02(2) and −0.01(2)].

CCDC reference number 186/1523.

See http://www.rsc.org/suppdata/dt/1999/2575/ for crystallographic files in .cif format.

Acknowledgements

This work was supported by a Grant-in-aid for Specially Promoted Research (09102004) from the Ministry of Education, Science, Sports and Culture, Japan.

References

1 R. H. Holm, S. Ciurli and J. A. Weigel, *Prog. Inorg. Chem.*, 1990, **38**, 1; B. Krebs and G. Henkel, *Angew. Chem., Int. Ed. Engl.*, 1991, **30**, 769; T. Shibahara, *Coord. Chem. Rev.*, 1993, **123**, 73; T. Saito, in *Early Transition Metal Clusters with* π*-Donor Ligands*, ed. M. H.

Chisholm, VCH, New York, 1995, ch. 3; I. Dance and K. Fisher, *Prog. Inorg. Chem.*, 1994, **41**, 637; P. Mathur, *Adv. Organomet. Chem.*, 1997, **41**, 243; H. Ogino, S. Inomata and H. Tobita, *Chem. Rev.*, 1998, **98**, 2093.

2 D. Coucouvanis, in *Molybdenum Enzymes, Cofactors, and Model Systems*, eds. E. I. Stiefel, D. Coucouvanis and W. E. Newton, American Chemical Society, Washington, DC, 1993, p. 304; J. B. Howard and D. C. Rees, *Chem. Rev.*, 1996, **96**, 2965; B. K. Burgess and D. J. Lowe, *Chem. Rev.*, 1996, **96**, 2983; D. Sellmann and J. Sutter, *Acc. Chem. Res.*, 1997, **30**, 460.

3 R. A. Sánchez-Delgado, *J. Mol. Catal.*, 1994, **86**, 287; C. Bianchini and A. Meli, *J. Chem. Soc.*, *Dalton Trans.*, 1996, 801; M. D. Curtis and S. H. Druker, *J. Am. Chem. Soc.*, 1997, **119**, 1027; C. Bianchini and A. Meli, *Acc. Chem. Res.*, 1998, **31**, 109.

4 (*a*) M. Hidai, Y. Mizobe and H. Matsuzaka, *J. Organomet. Chem.*, 1994, **473**, 1; (*b*) M. Hidai and Y. Mizobe, *ACS Symp. Ser.*, 1996, **653**, 310; (*c*) S. Kuwata, M. Andou, K. Hashizume, Y. Mizobe and M. Hidai, *Organometallics*, 1998, **17**, 3429; (*d*) S. Kuwata and M. Hidai, *Chem. Lett.*, 1998, 885; (*e*) Z. Tang, Y. Nomura, S. Kuwata, Y. Ishii, Y. Mizobe and M. Hidai, *Inorg. Chem.*, 1998, **37**, 4909; (*f*) J.-P. Qü, D. Masui, Y. Ishii and M. Hidai, *Chem. Lett.*, 1998, 1003; (*g*) Y. Mizobe, M. Hosomizu and M. Hidai, *Inorg. Chim. Acta*, 1998, **273**, 238; (*h*) T. Ikada, S. Kuwata, Y. Mizobe and M. Hidai, *Inorg. Chem.*, 1998, **37**, 5793; (*i*) S. Takemoto, S. Kuwata, Y. Nishibayashi and M. Hidai, *Inorg. Chem.*, 1998, **37**, 6428; (*j*) T. Sato, M. Nishio, Y. Ishii, H. Yamazaki and M. Hidai, *J. Organomet. Chem.*, 1998, **569**, 99; (*k*) T. Ikada, S. Kuwata, Y. Mizobe and M. Hidai, *Inorg. Chem.*, 1999, **38**, 64.

5 H. Matsuzaka, Y. Takagi and M. Hidai, *Organometallics*, 1994, **13**, 13; H. Matsuzaka, Y. Takagi, Y. Ishii, M. Nishio and M. Hidai, *Organometallics*, 1995, **14**, 2153; H. Shimada, J.-P. Qü, H. Matsuzaka, Y. Ishii and M. Hidai, *Chem. Lett.*, 1995, 671; Y. Nishibayashi, M. Yamanashi, Y. Takagi and M. Hidai, *Chem. Commun.*, 1997, 859; Y. Takagi, H. Matsuzaka, Y. Ishii and M. Hidai, *Organometallics*, 1997, **16**, 4445.

6 T. Murata, H. Gao, Y. Mizobe, F. Nakano, S. Motomura, T. Tanase, S. Yano and M. Hidai, *J. Am. Chem. Soc.*, 1992, **114**, 8287; T. Murata, Y. Mizobe, H. Gao, Y. Ishii, T. Wakabayashi, F. Nakano, T. Tanase, S. Yano, M. Hidai, I. Echizen, H. Nanikawa and S. Motomura, *J. Am. Chem. Soc.*, 1994, **116**, 3389; T. Wakabayashi, Y. Ishii, T. Murata, Y. Mizobe and M. Hidai, *Tetrahedron Lett.*, 1995, **36**, 5585; T. Wakabayashi, Y. Ishii, K. Ishikawa and M. Hidai, *Angew. Chem.*, *Int. Ed. Engl.*, 1996, **35**, 2123.

7 K. Hashizume, Y. Mizobe and M. Hidai, *Organometallics*, 1996, **15**, 3303.

8 (*a*) Z. Tang, Y. Nomura, Y. Ishii, Y. Mizobe and M. Hidai, *Organometallics*, 1997, **16**, 151; (*b*) Z. Tang, Y. Nomura, Y. Ishii, Y. Mizobe and M. Hidai, *Inorg. Chim. Acta*, 1998, **267**, 73; (*c*) D. Masui, Y. Ishii and M. Hidai, *Chem. Lett.*, 1998, 717.

9 C. K. Johnson, ORTEP II, Report ORNL-5138, Oak Ridge National Laboratory, Oak Ridge, TN, 1976.

10 A. Fumagalli, F. Demartin and A. Sironi, *J. Organomet. Chem.*, 1985, **279**, C33; D. Mani and H. Vahrenkamp, *Chem. Ber.*, 1986, **119**, 3649; H. Jungbluth, G. Süss-Fink, M. A. Pellinghelli and A. Tiripicchio, *Organometallics*, 1990, **9**, 1670; D. Carmona, J. Ferrer, A. Mendoza, F. J. Lahoz, J. Reyes and L. A. Oro, *Angew. Chem.*, *Int. Ed. Engl.*, 1991, **30**, 1171; G. Süss-Fink, S. Haak, V. Ferrand and H. Stoeckli-Evans, *J. Chem. Soc.*, *Dalton Trans.*, 1997, 3861; A. U. Härkönen, M. Ahlgrén, T. A. Pakkanen and J. Pursiainen, *Organometallics*, 1997, **16**, 689; V. Ferrand, G. Süss-Fink, A. Neels and H. Stoeckli-Evans, *J. Chem. Soc.*, *Dalton Trans.*, 1998, 3825; A. U. Härkönen, M. Ahlgrén, T. A. Pakkanen and J. Pursiainen, *J. Organomet. Chem.*, 1999, **573**, 225.

11 (*a*) A. M. Mueting, P. D. Boyle, R. Wagner and L. H. Pignolet, *Inorg. Chem.*, 1988, **27**, 271; (*b*) T. A. Bright, R. A. Jones, S. U. Koschmieder and C. M. Nunn, *Inorg. Chem.*, 1988, **27**, 3819; (*c*) A. Venturelli and T. B. Rauchfuss, *J. Am. Chem. Soc.*, 1994, **116**, 4824; (*d*) T. Nishioka and K. Isobe, *Chem. Lett.*, 1994, 1661; (*e*) W. D. Jones and R. M. Chin, *J. Am. Chem. Soc.*, 1994, **116**, 198; (*f*) D. A. Vicic and W. D. Jones, *Organometallics*, 1997, **16**, 1912.

12 J. R. Lockemeyer, T. B. Rauchfuss and A. L. Rheingold, *J. Am. Chem. Soc.*, 1989, **111**, 5733; K. Hashizume, Y. Mizobe and M. Hidai, *Organometallics*, 1995, **14**, 5367.

13 For example, (*a*) K. Moseley, J. W. Kang and P. M. Maitlis, *J. Chem. Soc. A*, 1970, 2875; (*b*) H. Werner, B. Heiser, B. Klingert and R. Dülfel, *J. Organomet. Chem.*, 1982, **240**, 179; (*c*) K. Tanaka, Y. Kushi, K. Tsuge, K. Toyohara, T. Nishioka and K. Isobe, *Inorg. Chem.*, 1998, **37**, 120.

14 H. Werner, *Angew. Chem.*, *Int. Ed. Engl.*, 1983, **22**, 927.

15 W. E. Watts, in *Comprehensive Organometallic Chemistry*, eds. G. Wilkinson, F. G. A. Stone and E. W. Abel, Pergamon, London, 1982, vol. 8, p. 1013.

16 L. Pauling, in *The Nature of the Chemical Bond*, 3rd edn., Cornell University Press, Ithaca, NY, 1960; A. Bondi, *J. Phys. Chem.*, 1964, **68**, 441.

17 M. Nishio and M. Hirota, *Tetrahedron*, 1989, **45**, 7201; M. Nishio, Y. Umezawa, M. Hirota and Y. Takeuchi, *Tetrahedron*, 1995, **51**, 8665.

18 R. O. Harris, N. K. Hota, L. Sadavoy and J. M. C. Yuen, *J. Organomet. Chem.*, 1973, **54**, 259.

19 P. S. Hallman, T. A. Stephenson and G. Wilkinson, *Inorg. Synth.*, 1972, **12**, 237.

20 P. J. Blower, J. R. Dilworth, J. P. Hutchinson and J. A. Zubieta, *J. Chem. Soc.*, *Dalton Trans.*, 1985, 1533.

21 TEXSAN, Crystal Structure Analysis Package, Molecular Structure Corp., The Woodlands, TX, 1985 and 1992.

22 PATTY, P. T. Beurskens, G. Admiraal, G. Beurskens, W. P. Bosman, S. Garcia-Granda, R. O. Gould, J. M. M. Smits and C. Smykalla, The DIRDIF program system, Technical Report of the Crystallography Laboratory, University of Nijmegen, 1992.

23 H. D. Flack, *Acta Crystallogr.*, *Sect. A*, 1983, **39**, 876.

Paper 9/02999K